Transcriptomic versus Chromosomal Prognostic Markers and Clinical Outcome in Uveal Melanoma

Lori A. Worley,[1] Michael D. Onken,[1] Erica Person,[1] Diane Robirds,[2] Julie Branson,[2] Devron H. Char,[3] Arie Perry,[2] and J. William Harbour[1]

Abstract

Purpose: To compare a gene expression – based classifier versus the standard genetic prognostic marker, monosomy 3, for predicting metastasis in uveal melanoma.

Experimental Design: Gene expression profiling, fluorescence *in situ* hybridization (FISH), and array comparative genomic hybridization (aCGH) were done on 67 primary uveal melanomas. Clinical and pathologic prognostic factors were also assessed. Variables were analyzed by Cox proportional hazards, Kaplan-Meier analysis, sensitivity, specificity, positive and negative predictive value, and positive and negative likelihood ratios.

Results: The gene expression – based molecular classifier assigned 27 tumors to class 1 (low risk) and 25 tumors to class 2 (high risk). By Cox univariate proportional hazards, class 2 signature ($P = 0.0001$), advanced patient age ($P = 0.01$), and scleral invasion ($P = 0.007$) were the only variables significantly associated with metastasis. Only the class 2 signature was needed to optimize predictive accuracy in a Cox multivariate model. A less significant association with metastasis was observed for monosomy 3 detected by aCGH ($P = 0.076$) and FISH ($P = 0.127$). The sensitivity and specificity for the molecular classifier (84.6% and 92.9%, respectively) were superior to monosomy 3 detected by aCGH (58.3% and 85.7%, respectively) and FISH (50.0% and 72.7%, respectively). Positive and negative predictive values (91.7% and 86.7%, respectively) and positive and negative likelihood ratios (11.9 and 0.2, respectively) for the molecular classifier were also superior to those for monosomy 3.

Conclusions: Molecular classification based on gene expression profiling of the primary tumor was superior to monosomy 3 and clinicopathologic prognostic factors for predicting metastasis in uveal melanoma.

In recent years, there has been increasing interest in individualized management of cancer patients based on predictive molecular testing (1, 2). Uveal (ocular) melanoma represents an ideal cancer for applying this strategy. Uveal melanoma is the most common primary cancer of the eye and has a strong predilection for hematogenous metastasis, particularly to the liver (3). Investigators have searched for clinical and pathologic prognostic factors for over a century and have identified several that are statistically associated with metastasis, including advanced patient age, anterior tumor location, increased tumor size, epithelioid cell type, and local tumor invasion through the sclera. However, predictive accuracy of these factors has not been adequate for making individualized clinical decisions, such as whether a given patient is at sufficiently high risk for metastasis to necessitate more intense and frequent metastatic surveillance or whether prophylactic systemic therapy may be appropriate. More recently, investigators have identified genetic alterations, such as monosomy 3, which are significantly associated with metastasis (4–6). With the development of more precise techniques for detecting chromosomal alterations, such as spectral karyotyping, fluorescence *in situ* hybridization (FISH), and comparative genomic hybridization (CGH), monosomy 3 has shown predictive accuracy superior to previous clinical and pathologic features (7–11).

Consequently, detection of monosomy 3 has now been adopted by most centers around the world as the gold standard for metastatic prediction in uveal melanoma (11–14). Indeed, prospective clinical trials are in the planning stages around the world that intend to use monosomy 3 as an entry criterion for preemptive antimetastatic interventions in high-risk uveal melanoma patients. However, the sensitivity

and specificity of monosomy 3, essential indicators of its utility as a clinical marker of metastatic risk, have not been reported, and it is possible that other available molecular classifiers may be superior to monosomy 3 for individualized patient management.

We and others recently reported a molecular classification of uveal melanomas based on gene expression profile that strongly predicts metastasis (15, 16). Tumors with the class 1 gene expression signature have a low risk of metastasis, and those with the class 2 signature have a high risk of metastasis (15). Our initial study was done on tumor tissue obtained after eye removal, but we have also shown that gene expression profiling can be done accurately on fine-needle biopsy specimens obtained before radiotherapy in uveal melanoma patients who do not require eye removal (17). Although these initial studies showed a strong association between the class 2 signature and monosomy 3, the former seemed to be superior in prognostic accuracy (15).

In this study of 67 uveal melanoma patients, the largest outcome study of its kind to date in uveal melanoma, we compare the prognostic accuracy of the gene expression–based classifier versus monosomy 3 detected by FISH and CGH.

Materials and Methods

Preparation of RNA and DNA. This study was approved by the Human Studies Committee at Washington University (St. Louis, MO), and informed consent was obtained from each subject. Tumor tissue was obtained immediately after eye removal, snap frozen, and prepared for RNA and DNA analysis as described previously (15). Genomic DNA was prepared using the Wizard Genomic DNA Purification kit (Promega, Madison, WI). RNA was isolated using PicoPure kits (Arcturus, Sunnyvale, CA). Complementary DNA was generated from total RNA by reverse transcription, linear amplification, and *in vitro* transcription to generate biotinylated cRNA targets that were hybridized to Affymetrix Hu133A and Av2 GeneChips according to the manufacturer's protocols with the assistance of the Siteman Cancer Center GeneChip Facility. Alternatively, some RNA samples were hybridized to Illumina Human Ref8 BeadChip arrays with the assistance of the Microarray Facility of the Washington University Genome Sequencing Center.

Microarray expression profiling. Microarray gene expression values were obtained on Affymetrix U133A, U133Av2, and Illumina Ref8 chips. Analysis of Affymetrix data was described previously (15, 17, 18). Illumina data were normalized by the rank invariant method using BeadStation software,[4] log2 transformed, and analyzed by principal component analysis using Spotfire software.[5] Assignment of tumors to class 1 and class 2 was done by a weighted voting algorithm using GeneCluster2 software[6] as described previously (15, 17).

Fluorescence in situ hybridization. Dual-color FISH was done as described previously (19). Briefly, paraffin-embedded tissue sections were deparaffinized with Citrisolv (Fisher Scientific, Pittsburgh, PA), dehydrated in 100% ethanol, subjected to target retrieval by steam heating in citrate buffer (pH 6.0) for 20 min, digested in pepsin solution (4 mg/mL in 0.9% NaCl) for 20 min at 37°C, rinsed in 2× SSC (300 mmol/L sodium chloride and 30 mmol/L sodium citrate) at room temperature for 5 min, and air dried. A Spectrum Green–labeled chromosome 7 centromeric DNA probe, CEP7(D7Z1) (Vysis, Inc., Downers Grove, IL), was paired with a Spectrum Orange–labeled

chromosome 3 centromeric probe, CEP3(D3Z1) (Vysis). Probes were diluted 1:50 in *t*-DenHyb buffer (Insitus Laboratories, Albuquerque, NM). Hybridization mix was applied to sections followed by denaturation in a 90°C slide moat (Boekel Scientific, Feasterville, PA) for 13 min. Hybridization was done overnight at 37°C in a humidified chamber. Slides were then washed in 50% formamide/1× SSC for 5 min and then twice in 2× SSC for 10 min each at room temperature. Slides were allowed to air dry, and then, nuclei were counterstained with 4′,6-diamidino-2-phenylindole (Insitus Laboratories). Sections were visualized on an Olympus BX60 fluorescent microscope (Olympus, Melville, NY). At least 100 nuclei were analyzed for each tumor. A threshold of 30% nuclei with one chromosome 3 signal and two chromosome 7 signals was established for making the call of monosomy 3.

Array CGH. Array CGH (aCGH) was done using human bacterial artificial chromosome arrays. Previously published samples were analyzed by the Microarray Shared Resource at the Comprehensive Cancer Center, University of California (San Francisco, CA) using a microarray-based platform containing a genome-wide collection of genomic contigs as described previously (15, 20). Newer, previously unpublished samples were analyzed by the Microarray and Genomics Facility of the Roswell Park Cancer Institute (Buffalo, NY) using an array platform containing ∼6,000 bacterial artificial chromosome clones.[7] One microgram of reference and test sample genomic DNA were individually fluorescently labeled using the BioArray CGH Labeling System (Enzo Life Sciences, Farmingdale, NY). DNA was hybridized to the arrays for 16 h at 55°C using a GeneTAC hybridization station (Genomic Solutions, Inc., Ann Arbor, MI). The hybridized aCGH slides were then scanned using a GenePix 4200A Scanner (Molecular Devices, Sunnyvale, CA) to generate high-resolution (5 μm) images for both Cy3 (test) and Cy5 (control) channels. Image analysis was done using the ImaGene (version 6.0.1) software from BioDiscovery, Inc. (El Segundo, CA). A loess-corrected log2 ratio of the background-subtracted test/control was calculated for each clone to compensate for nonlinear raw aCGH profiles in each sample. A log2 average raw ratio of >0.5 was used as the threshold for significant DNA copy number deviations.

Statistical analysis. Fisher's exact test was used to assess the significance of association between two categorical variables. Cox univariate proportional hazards was used to assess time-dependent association with metastasis for categorical and continuous variables. Kaplan-Meier analysis was used to assess time-dependent association with metastasis for categorical variables. Continuous variables were dichotomously categorized by the value that maximized sensitivity and specificity by receiver operating characteristics analysis. Variables that exhibited a significant association with metastasis were further analyzed by Cox multivariate proportional hazards modeling to assess their relative contribution to metastasis. Sensitivity, specificity, likelihood ratios, and predictive values were assessed for all clinical, pathologic, and molecular factors. In analysis A, metastasis was used as the end point. In analysis B, class 2 gene expression profile was used as a surrogate end point in metastasis-free patients. All statistical analyses were done using MedCalc software version 9.0.0.1.

Results

The study included 67 uveal melanoma patients treated by enucleation. Table 1 summarizes the clinical and pathologic features. Gene expression profiling was done on 52 tumors, including 26 analyzed with the Affymetrix GeneChip array, 16 with the Illumina Ref8 BeadChip array, and 10 with both platforms. Tumors analyzed on the Affymetrix platform were previously assigned to class 1 or class 2 (15, 17). In a similar

---

[4] http://www.illumina.com
[5] http://www.spotfire.com
[6] http://www.broad.mit.edu/cancer/software

[7] http://microarrays.roswellpark.org

Table 1. Summary of clinical and pathologic features

Clinicopathologic factors (*N* = 67 patients)	
Age at diagnosis, mean (range)	60.6 (24-87)
Gender, *n* (%)	
Male	44 (66)
Female	23 (34)
Eye, *n* (%)	
Right	36 (54)
Left	31 (46)
Tumor location, *n* (%)	
Posterior	40 (59)
Anterior	27 (41)
Largest tumor diameter (mm), mean (range)	17.4 (5.4-24)
Tumor thickness (mm), mean (range)	9.7 (2.2-22)
Histopathologic cell type, *n* (%)	
Spindle	23 (34)
Mixed	21 (31)
Epithelioid	23 (34)
Histopathologic local invasion, *n* (%)	
None	31 (46)
Intrascleral	19 (28)
Extrascleral	17 (25)
Metastasis	18 (27)
Months from diagnosis to end point, mean (range)	28.4 (1-90)

manner, the 26 tumors analyzed on the Illumina platform were assigned to one of the two classes (Fig. 1A). Using a weighted voting predictive algorithm and 4-fold cross-validation, accurate class assignment was achieved with as few as 7 genes from a 40-gene signature that we previously validated on four independent data sets (Fig. 1B and C). Altogether, 27 tumors were assigned to class 1 and 25 tumors were assigned to class 2. In the 10 tumors analyzed by both the Affymetrix and Illumina platforms, there was 100% agreement in class assignments between the two platforms (*P* = 0.004, Fisher's exact test). Chromosome 3 status was assessed by FISH and aCGH. Monosomy 3 was detected in 21 of 49 (43%) tumors by aCGH and in 13 of 36 (36%) tumors by FISH (Fig. 2). The gene expression classifier results were significantly associated with monosomy 3 by both aCGH (*P* = 4.1×10^{-6}, Fisher's exact test) and FISH (*P* = 0.009).

By Cox univariate proportional hazards, class 2 gene expression profile (*P* = 0.0001), advanced patient age (*P* = 0.01), and scleral invasion (*P* = 0.007) were significantly associated with metastasis (Table 2). Kaplan-Meier analysis rendered similar results. When all three significant variables were entered into a Cox multivariate model, only class 2 gene expression profile exhibited significant association with metastasis.

Sensitivity, specificity, likelihood ratios, and predictive values were calculated for each clinical, pathologic, and molecular prognostic factor (Supplementary Table S1). In analysis A, the metastasis group consisted of all 18 patients who had developed metastasis, and the nonmetastasis group contained all 16 patients without metastasis who had at least 3-year follow-up after ocular tumor treatment. The class 2 gene expression profile outperformed all other prognostic variables, with 84.6% sensitivity and 92.9% specificity (Table 3). Similar results were obtained when the nonmetastasis group was limited to metastasis-free patients with at least 4-year follow-up (data not shown). The other predictive indices for gene
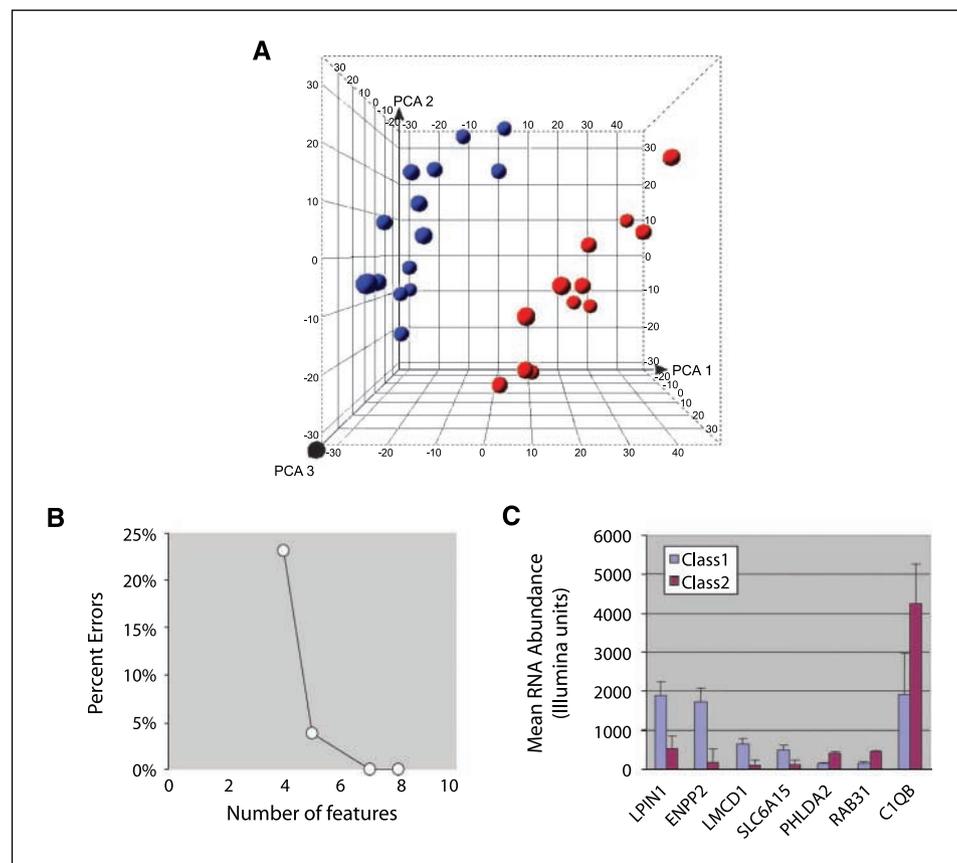
Fig. 1. Gene expression profiling of 26 uveal melanomas using the Illumina Human Ref8 platform. *A,* gene expression profiles of 26 primary uveal melanomas (spheres) displayed in three-dimensional space by principal component analysis to show the clustering of tumors into class 1 (*blue*) and class 2 (*red*) tumors. *B,* performance of a weighting voting classifier using 4-fold cross-validation. Percentage classification errors are a function of the number of features (genes) in the predictor. Maximum accuracy was achieved with seven genes. *C,* mean RNA expression of the seven genes in the weighted voting predictor in 14 class 1 tumors and 12 class 2 tumors.

Fig. 2. Assays for detecting monosomy 3. *A,* representative examples of tumors analyzed by aCGH exhibiting disomy 3 and monosomy 3. X axis, distribution of chromosome 3 fragments (represented in bacterial artificial chromosomes) distributed along the chromosome; Y axis, relative proportion of tumor DNA compared with normal control DNA, expressed as the log2 ratio, where 0 indicates [tumor DNA] = [normal DNA], a negative value indicates [tumor DNA] ‹ [normal DNA], and a positive value indicates [tumor DNA] › [normal DNA]. Normal DNA was derived from peripheral blood lymphocytes from the same patient. *B,* left, summary of FISH results. The graph plots the percentage of nuclei exhibiting one chromosome 3 signal (*red*) and two chromosome 7 signals (*green*). The 30% threshold for monosomy 3 is indicated. Right, representative photomicrographs of FISH analysis in disomy 3 and monosomy 3 tumors. Note that some tumor nuclei in the monosomy 3 tumor exhibit two red signals (*arrow*), indicating heterogeneity for monosomy 3.
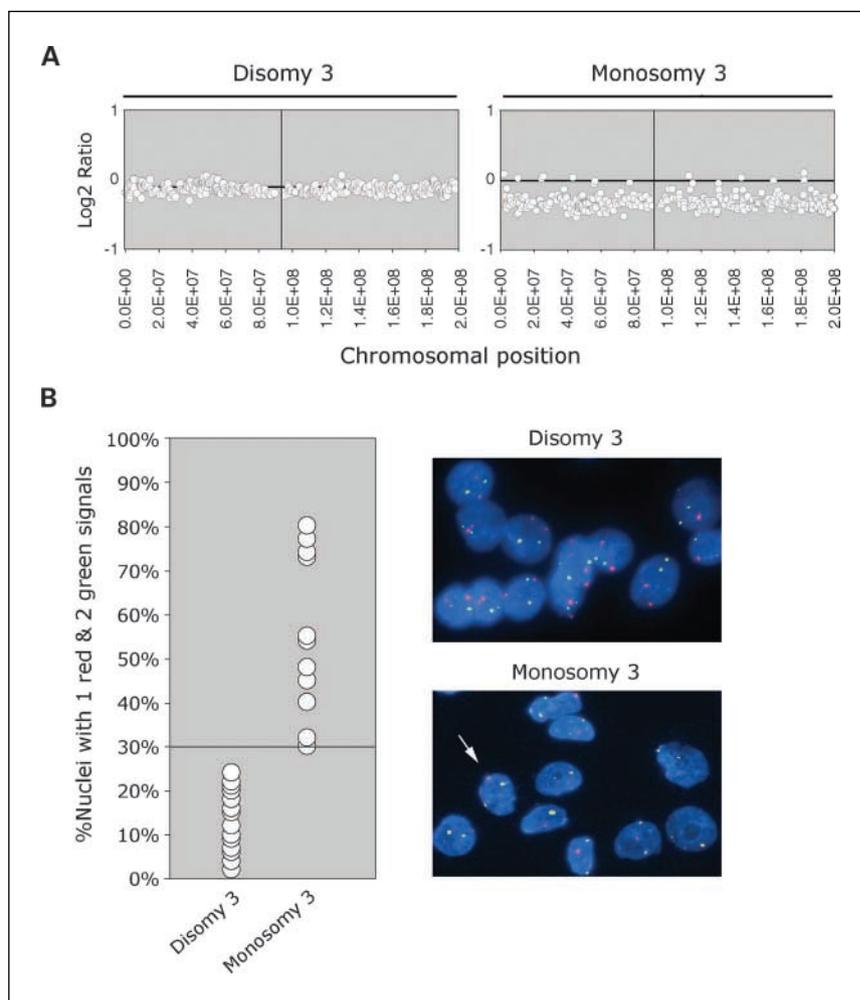
expression profiling were also greatly superior to those for other clinical, pathologic, and molecular features, with positive and negative predictive values of 91.7% and 86.7%, respectively, and positive and negative likelihood ratios of 11.9 and 0.2, respectively.

In analysis B, the number of patients available for evaluation was expanded to 59 by using the gene expression profile as a surrogate end point in metastasis-free patients with less than 3-year follow-up (i.e., class 1 tumors were assigned to the "nonmetastasis" group and class 2 tumors to the "metastasis" group). The most accurate predictive factors were monosomy 3

detected by aCGH (73.1% sensitivity, 85.7% specificity), monosomy 3 detected by FISH (55.6% sensitivity, 85.7% specificity), and scleral invasion (40.6% sensitivity, 92.3% specificity).

Discussion

In this study, the gene expression–based classifier predicted metastasis more accurately than clinicopathologic features and monosomy 3, assessed either by the widely used FISH method or by the more quantitative aCGH technique. This finding has

Table 2. Summary of survival analysis

	Cox univariate	Cox multivariate	Kaplan-Meier
Class 2 gene expression profile	0.0001	0.0449	0.0001
Monosomy 3 (aCGH)	0.0762	—	0.0856
Monosomy 3 (FISH)	0.1275	—	0.1482
Age	0.0144	0.4703	0.007
Scleral invasion	0.0071	0.2372	0.0119
Histopathologic cell type	0.2802	—	0.1126
Tumor thickness	0.1085	—	0.1096
Gender	0.4184	—	0.4086
Largest tumor diameter	0.5867	—	0.5899
Anterior tumor location	0.4939	—	0.5018

Table 3. Predictive accuracy of clinical, pathologic, and molecular prognostic features

Prognostic factor	Sensitivity	Specificity	Positive likelihood ratio	Negative likelihood ratio	Positive predictive value	Negative predictive value
Analysis A (*n* = 35)						
Class 2 gene expression profile	84.6	92.9	11.9	0.2	91.7	86.7
Monosomy 3 (aCGH)	58.3	85.7	4.1	0.5	77.8	70.6
Monosomy 3 (FISH)	50.0	72.7	1.8	0.7	62.5	61.5
Scleral invasion	44.4	93.7	7.1	0.6	88.9	60.0
Age	72.2	68.7	2.3	0.4	72.2	68.8
Anterior tumor location	38.9	75.0	1.6	0.8	63.6	52.2
Mixed or epithelioid cell type	77.8	50.0	1.6	0.4	63.6	66.7
Largest tumor diameter <18.9 mm	58.8	62.5	1.6	0.7	62.5	58.8
Gender	72.2	37.5	1.2	0.7	56.5	54.5
Tumor thickness <8.1 mm	52.9	93.7	8.5	0.5	90.0	65.2
Analysis B (*n* = 59)						
Monosomy 3 (aCGH)	73.1	85.7	5.1	0.3	86.4	72.0
Monosomy 3 (FISH)	55.6	85.7	3.9	0.5	83.3	60.0
Scleral invasion	40.6	92.3	5.3	0.6	86.7	55.8
Age	56.2	73.1	2.1	0.6	72.0	57.6
Mixed or epithelioid cell type	81.2	53.8	1.8	0.4	68.4	70.0
Tumor thickness <11.3 mm	77.4	46.2	1.4	0.5	63.2	63.2
Gender	46.9	65.4	1.4	0.8	62.5	50.0
Anterior tumor location	79.3	36.0	1.2	0.6	59.0	60.0
Largest tumor diameter >15 mm	71.9	30.8	1.0	0.9	56.1	47.1

important implications for patient care and future research because the vast majority of investigators currently use monosomy 3 as the standard for molecular prediction in uveal melanoma (12, 13). In contrast to the experience in some other cancers, gene expression profiling in uveal melanoma is extremely robust and reproducible on independent data sets and different analytic platforms, including Affymetrix and Illumina microarray chips and quantitative PCR (15–18, 21). As few as 7 genes from our 40-gene signature, which previously was validated on four independent Affymetrix data sets (17), were sufficient for accurately classifying all 26 tumors analyzed on the Illumina platform. The binary classifier has been verified independently by other investigators (16) and can be done accurately and reproducibly on fine-needle biopsy specimens (17). Thus, gene expression profiling is clinically feasible not only for the ~10% of cases that require enucleation but also for the vast majority that are treated with radiotherapy and other globe-sparing methods.

There are several potential explanations for the superiority of gene expression profiling over monosomy 3. From a technical standpoint, FISH is more challenging in uveal melanoma than in some other cancers due to its dense cellularity and elongated nuclei that weave in and out of the plane of section. The former makes it difficult to establish which signals belong to which cells, whereas the latter increases the likelihood of under-estimating signal counts (false negatives). To complicate this problem, monosomy 3 is usually heterogeneous within a given tumor (Fig. 2B). Consequently, the percentage of nuclei with one chromosome 3 that is set as a threshold for calling the tumor monosomy 3 is somewhat arbitrary and may lead to false negatives or false positives. This heterogeneity for monosomy 3 can also lead to sampling error. In contrast, we have not found heterogeneity in the gene expression profile when multiple areas of the same tumor are sampled (data not shown). Although these pitfalls are partially overcome by using fresh cytologic preparations rather than paraffin-embedded

tissue (data not shown), there are still artifacts that hinder interpretation. Most notable is the tendency for signal splitting (appearance of two closely positioned signals at the site of a single centromere), which is common with the chromosome 3 probe. For reasons that are unclear, this phenomenon is variable and is more prominent in some specimens than others, leading to potential overestimation of centromere numbers. In addition to these problems, some tumors sustain interstitial deletions on chromosome 3 rather than loss of the whole chromosome (22), which likely would be undetected by FISH, leading to false-negative calls.

Because of these shortcomings of FISH, we also assessed chromosome 3 status by aCGH, which is a quantitative technique that overcomes many of the technical obstacles of FISH. Nevertheless, the performance of aCGH was still inferior to gene expression profiling. This may be due, at least in part, to the inability of aCGH to detect isodisomy 3, which occurs in some uveal melanomas when there is loss of one chromosome 3 and duplication of the remaining, presumably abnormal chromosome 3 (23). In addition, it seems likely that gene expression profiling represents a "snapshot" that captures more of the functional complexity of the tumor vis-à-vis metastatic potential than does a simple chromosomal marker, such as monosomy 3. Consistent with this idea, we recently showed that the gene expression pattern exhibited by the class 2 tumors was consistent with a primordial, epithelial-like phenotype, which may indicate that class 2 tumors contain more stem-like cancer cells with increased metastatic capacity (18).

Based on these results, plans are under way to optimize and validate the molecular classifier on a larger patient population. Ultimately, this classifier could be used to individualize the intensity and frequency of metastatic surveillance and to guide entry of high-risk patients into clinical trials of preemptive antimetastatic therapies, such as vaccines and targeted molecular agents.

References

1. Taylor JM, Yu M, Sandler HM. Individualized predictions of disease progression following radiation therapy for prostate cancer. J Clin Oncol 2005;23:816–25.

2. Efferth T, Volm M. Pharmacogenetics for individualized cancer chemotherapy. Pharmacol Ther 2005; 107:155–76.

3. Harbour JW. Clinical overview of uveal melanoma: introduction to tumors of the eye. In: Albert DM, Polans A, editors. Ocular oncology. New York: Marcel Dekker; 2003. p. 1–18.

4. Sisley K, Rennie IG, Cottam DW, Potter AM, Potter CW, Rees RC. Cytogenetic findings in six posterior uveal melanomas: involvement of chromosomes 3, 6, and 8. Genes Chromosomes Cancer 1990;2:205–9.

5. Prescher G, Bornfeld N, Becher R. Nonrandom chromosomal abnormalities in primary uveal melanoma. J Natl Cancer Inst 1990;82:1765–9.

6. Horsman DE, Sroka H, Rootman J, White VA. Monosomy 3 and isochromosome 8q in a uveal melanoma. Cancer Genet Cytogenet 1990;45:249–53.

7. McNamara M, Felix C, Davison EV, Fenton M, Kennedy SM. Assessment of chromosome 3 copy number in ocular melanoma using fluorescence *in situ* hybridization. Cancer Genet Cytogenet 1997; 98:4–8.

8. Gordon KB, Thompson CT, Char DH, et al. Comparative genomic hybridization in the detection of DNA copy number abnormalities in uveal melanoma. Cancer Res 1994;54:4764–8.

9. Naus NC, van Drunen E, de Klein A, et al. Characterization of complex chromosomal abnormalities in uveal melanoma by fluorescence *in situ* hybridization, spectral karyotyping, and comparative genomic hybridization. Genes Chromosomes Cancer 2001;30: 267–73.

10. Prescher G, Bornfeld N, Hirche H, Horsthemke B, Jockel KH, Becher R. Prognostic implications of monosomy 3 in uveal melanoma. Lancet 1996;347: 1222–5.

11. Kilic E, van Gils W, Lodder E, et al. Clinical and cytogenetic analyses in uveal melanoma. Invest Ophthalmol Vis Sci 2006;47:3703–7.

12. Patel KA, Edmondson ND, Talbot F, Parsons MA, Rennie IG, Sisley K. Prediction of prognosis in patients with uveal melanoma using fluorescence *in situ* hybridisation. Br J Ophthalmol 2001;85:1440–4.

13. Midena E, Bonaldi L, Parrozzani R, Tebaldi E, Boccassini B, Vujosevic S. *In vivo* detection of monosomy 3 in eyes with medium-sized uveal melanoma using transscleral fine needle aspiration biopsy. Eur J Ophthalmol 2006;16:422–5.

14. Sandinha MT, Farquharson MA, McKay IC, Roberts F. Monosomy 3 predicts death but not time until death in choroidal melanoma. Invest Ophthalmol Vis Sci 2005;46:3497–501.

15. Onken MD, Worley LA, Ehlers JP, Harbour JW. Gene expression profiling in uveal melanoma reveals two molecular classes and predicts metastatic death. Cancer Res 2004;64:7205–9.

16. Tschentscher F, Husing J, Holter T, et al. Tumor classification based on gene expression profiling shows that uveal melanomas with and without monosomy 3 represent two distinct entities. Cancer Res 2003;63:2578–84.

17. Onken MD, Worley LA, Davila RM, Char DH, Harbour JW. Prognostic testing in uveal melanoma by transcriptomic profiling of fine needle biopsy specimens. J Mol Diagn 2006;8:567–73.

18. Onken MD, Ehlers JP, Worley LA, Makita J, Yokota Y, Harbour JW. Functional gene expression analysis uncovers phenotypic switch in aggressive uveal melanomas. Cancer Res 2006;66:4602–9.

19. Perry A, Roth KA, Banerjee R, Fuller CE, Gutmann DH. NF1 deletions in S-100 protein-positive and negative cells of sporadic and neurofibromatosis 1 (NF1)-associated plexiform neurofibromas and malignant peripheral nerve sheath tumors. Am J Pathol 2001; 159:57–61.

20. Pinkel D, Segraves R, Sudar D, et al. High resolution analysis of DNA copy number variation using comparative genomic hybridization to microarrays. Nat Genet 1998;20:207–11.

21. Onken MD, Lin AY, Worley LA, Folberg R, Harbour JW. Association between microarray gene expression signature and extravascular matrix patterns in primary uveal melanomas. Am J Ophthalmol 2005; 140:748–9.

22. Cross NA, Ganesh A, Parpia M, Murray AK, Rennie IG, Sisley K. Multiple locations on chromosome 3 are the targets of specific deletions in uveal melanoma. Eye 2006;20:476–81.

23. White VA, McNeil BK, Thiberville L, Horsman DE. Acquired homozygosity (isodisomy) of chromosome 3 during clonal evolution of a uveal melanoma: association with morphologic heterogeneity. Genes Chromosomes Cancer 1996;15:138–43.